Acta Materialia 277 (2024) 120195

Contents lists available at ScienceDirect

Acta Materialia

journal homepage: www.elsevier.com/locate/actamat

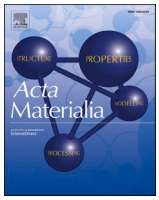

Full length article

Effect of deformation on the bainitic transformation

Imed-Eddine Benrabah [a,b,*], Arina Deboer [b], Guillaume Geandier [a], Hugo Van Landeghem [c], Christopher Hutchinson [d,1], Yves Brechet [d], Hatem Zurob [b]

[a] Université de Lorraine, CNRS, IJL, F-54000 Nancy, France
[b] Department of Materials Science and Engineering, McMaster University, Hamilton, ON, Canada
[c] SIMaP, University Grenoble Alpes, CNRS, Grenoble INP, Grenoble F-38000, France
[d] Department of Materials Science and Engineering, Monash University, Clayton, VIC 3800, Australia

ARTICLE INFO

Keywords:
Bainitic Ferrite
Effect of deformation
Ausforming
Dynamic transformation

ABSTRACT

The effect of deformation on the growth kinetics of bainitic ferrite plates was investigated under two types of conditions. In the first, deformation (ausforming) precedes the austenite-to-bainite transformation, while in the second case the phase transformation and deformation occur concurrently. The results clearly demonstrate that ausforming accelerates the nucleation of bainitic ferrite plates, leading to significant refinement of the final microstructure. When the bainite transformation takes place during deformation, the effect on nucleation was less obvious, but a clear increase in the growth rate of bainitic ferrite was observed. A modified version of the Zener-Hillert model for plate growth, with adjustments that allow for incorporating the effect of defects in the matrix and the effect of applied deformation on the movement of interfacial disconnections, was used to rationalize the effect of deformation on the growth kinetics. The calculations show that after ausforming, the stored dislocations act as a barrier to the growth of bainitic ferrite plates, resulting in a decreased lengthening rate. Conversely, when the transformation occurs concurrently with deformation, the lengthening rate of bainitic ferrite plates is accelerated due to the interaction between the applied stress and the disconnections at the tip of the bainitic ferrite plates.

1. Introduction

The effect of deformation on the bainitic phase transformation and plate-like ferrite growth in general, has been extensively reported in the literature [1–11]. The ausforming process, where austenite is subjected to plastic deformation before the onset of the phase transformation, has a significant impact on the kinetics of the transformation and the final mechanical properties of the material. Ausforming has been used to design novel grades of steel that possess both ultrahigh strength and excellent toughness [12]. The bainitic ferrite that grows from deformed austenite inherits the high dislocation density of the deformed structure, leading to increased strength [13]. Hu et al. [4] used dilatometry to investigate the bainitic transformation kinetics following ausforming at different temperatures and found that the transformation was accelerated during the initial stage, but the final fraction was reduced. However, they also reported that ausforming at high temperatures could lead to a retardation of the transformation. Similarly, Singh et al. [14] suggested that the rate of nucleation of bainitic ferrite is enhanced due to ausforming, but the lengthening of the plates is retarded by prior deformation. Gong et al. [15] used in situ neutron diffraction to demonstrate that ausforming at 300 °C resulted in a faster overall bainitic transformation. These studies offer consistent evidence of the acceleration of nucleation due to the elevated dislocation density in austenite, and a retardation of growth due to the mechanical stabilization of austenite and/or the presence of dislocations in the matrix which can hinder the movement of the transformation interface [16]. Very few studies have attempted to model the effect of ausforming on the bainitic transformation. A quantitative model of the effect of prior deformation on the bainitic transformation would greatly aid alloy development by permitting engineers to compute deformation-Continuous Cooling Transformation (CCT) curves. Chatterjee et al. [17] proposed an energy balance-based theory to predict austenite stabilization under strain and its impact on the bainitic transformation but did not address the kinetics of the phase transformation. Kumnorkaew et al. [18] and Zolotorevsky

* Corresponding author at: Université de Lorraine, CNRS, IJL, F-54000 Nancy, France.
E-mail address: imed-eddine.benrabah@univ-lorraine.fr (I.-E. Benrabah).

[1] Christopher Hutchinson was an Editor of the journal during the review period of the article. To avoid a conflict of interest, Christopher Hutchinson was blinded to the record and another editor processed this manuscript.

https://doi.org/10.1016/j.actamat.2024.120195
Received 18 March 2024; Received in revised form 30 June 2024; Accepted 13 July 2024
Available online 19 July 2024

et al. [19] extended the displacive model proposed by Van Bohemen and Sietsma [20] to describe the effect of ausforming on the rate of bainitic transformation under isothermal conditions and continuous cooling, respectively. In these models, the introduction of dislocations by deformation enhances both the austenite stability and the bainite nucleation rate, and the overall transformation rate is determined by the balance between the two effects.

It is also interesting to consider the formation of ferrite and bainitic ferrite concurrently with the plastic deformation of austenite [8,9, 21–23]. Some researchers have suggested that the dynamic transformation may contribute to microstructure evolution during the thermomechanical processing of advanced high strength steels [24]. An applied stress during the austenite to ferrite transformation has been shown to accelerate the transformation kinetics in several studies [8,21, 22,25]. Shibata et al. [8] used in-situ neutron diffraction analysis to investigate the dynamic ferrite transformation in Fe-C-2Mn and Fe-C-10Ni alloys at temperatures below Ae_3 and found that the transformation rate was accelerated by the applied deformation. The bainitic transformation was investigated by Bevilaqua et al. [21], where the authors used in-situ high energy synchrotron X-ray diffraction measurements to examine this effect at 500 °C and observed a significant acceleration of the bainitic transformation rate during deformation. Shipway et al. [6] reported that even a compressive stress with a magnitude lower than the yield stress of austenite could lead to an acceleration of the bainitic transformation. However, these studies did not clarify whether the observed acceleration was due to an increase in the nucleation rate, the growth rate, or both. The transformation acceleration was mainly explained in the literature by the introduction of defects in the austenite during deformation leading to an increase in the nucleation rate [21,26]. Others argued that the mechanical force can be added to the driving force of the transformation thus accelerating the growth of the bainite plates [6]. Here again, there have been very few attempts to quantitatively model the impact of deformation on the kinetics of the bainitic transformation. The studies presented above suggest that the interaction between deformation and phase transformation is complex. The effect of deformation may depend on the stress state, the applied strain and the strain rate. In addition, the interaction may depend on composition and the presence and/or concurrent precipitation of carbides or other phases. Separating these effects can be challenging and often necessitates a large number of experiments. Moreover, certain interdependencies, such as those between strain, stress, and strain rate, may make isolating individual effects difficult or even impossible in some cases [27].

The present authors have developed a new model to describe plate-like ferrite growth kinetics during isothermal holding [28]. The model is based on the Zener-Hillert [29] diffusional growth theory, with the incorporation of a barrier energy, arising from the interaction between the moving interface and the defects present in the matrix. Using this approach, the authors were able to predict the magnitude of the barrier and good agreement was obtained between the predicted and measured plate lengthening kinetics for different steels. In this paper, the authors will demonstrate an extension of this model and use it to describe the effect of applied deformation on the bainitic transformation.

In order to test the model predictions, the impact of deformation on bainite growth kinetics will be investigated using in-situ high energy X-ray diffraction (HEXRD) to monitor the transformation under different deformation modes: (i) the deformation-free case, (ii) ausforming, and (iii) the dynamic transformation case in which bainite is formed while the sample is being deformed. HEXRD allows for the real-time tracking of ferrite fraction evolution with great precision. By combining this technique with microstructural observation, the study provides insights into the effect of applied deformation on the transformation behaviour. The predictions of the model will be compared with the experimental observations.

2. Materials and methods

The steel investigated in the present contribution has a chemical composition of Fe-0.38C–0.89Mn–1.42Si–0.89Cr–0.25Mo–0.08 V (wt. %). The steel was cast in the form of a 50 kg ingot at CanmetMATERIALS (Hamilton, Canada) and hot rolled above 900 °C, down to a thickness of 3 cm, followed by accelerated water cooling. The Bs (bainite start) temperature of the steel was calculated to be 540 °C [30].

2.1. High energy X-Ray diffraction experiments

The bainitic transformation kinetics during the thermo-mechanical treatments were studied using high energy x-ray diffraction. The experiments were conducted at the DESY synchrotron in Hamburg, Germany, on the PETRA III P07 beamline. Thermo-mechanical treatments were carried in a modified 805 DIL Bahr deformation dilatometer, equipped with induction heating system and a deformation unit (Fig. 1-a). The dilatometer is equipped with windows that allow the X-Ray beam to pass in between the turnings of the heating coil and interact only with the sample. Cylindrical samples of 5 mm diameter and 10 mm length were used for testing (Fig. 1-a). The dilatometer uses an induction coil to heat the sample and allows real time temperature monitoring via an S-type thermocouple, welded at the centre of the sample. To prevent oxidation and decarburization of the heated steels, the experiments were conducted under a vacuum of 10^{-4} bar. The experiments were carried out using a monochromatic beam energy of 103 keV, which corresponds to a wavelength of $1.197.10^{-11}$ m and using a beam size of 800×800 μm^2. A PerkinElmer detector was used to gather full frame data and was positioned 1.34 m away from the sample with the direct beam centered on the 2D detector to obtain full diffraction rings (4 for each main phase). Patterns were recorded at a frequency of 10 Hz, i.e., one image every 0.1 s. Calibration was performed using a LaB6 standard.

Three scenarios were analyzed to assess the effect of deformation, as shown in Fig. 1-b. The first scenario involved the bainitic transformation without any deformation. The second scenario, which will be referred to as ausforming, investigated the effect of prior deformation on subsequent transformation kinetics. The third scenario, which will be referred to as dynamic transformation, involved continuous deformation of the sample and the formation of bainite during deformation.

The samples were first heated to a temperature of 900 °C, to achieve a completely austenitic microstructure. Subsequently, the samples were rapidly cooled to various temperatures below the Bs temperature (400 °C, 450 °C, and 500 °C) at a cooling rate of 90 K/s. For the first scenario (no deformation), the samples were held for 5 min at the transformation temperature prior to being quenched to room temperature using Argon gas. For the ausforming experiments, the samples were deformed, immediately upon reaching the holding temperature. The strain rate used was $0.1s^{-1}$ and the total strains were 0.1 and 0.2, as shown in Fig. 1-b. To investigate the dynamic austenite-to-bainite transformation, the samples were deformed at a strain rate of 0.001 s^{-1} up to a strain of 0.2 at the isothermal holding temperature, Fig. 1-c.

2.2. HEXRD data analysis

The acquired two-dimensional (2D) Debye-Scherer rings were analyzed using pyFAI software package and integrated over the whole azimuthal range to generate one-dimensional (1D) diffraction patterns (intensity vs 2θ), as shown in Fig. 2. The generated 1D patterns were then quantitatively analyzed to extract phase fraction evolution during the applied treatments of the material.

The lattice parameters and phase fractions were determined using the standard sequential Rietveld method, conducted using the FullProf software [31]. This method involves refining the diffraction patterns to obtain the best possible match between the observed and calculated patterns. The volume fractions of austenite and ferrite were calculated at each time step of the whole thermo-mechanical treatment. The carbon

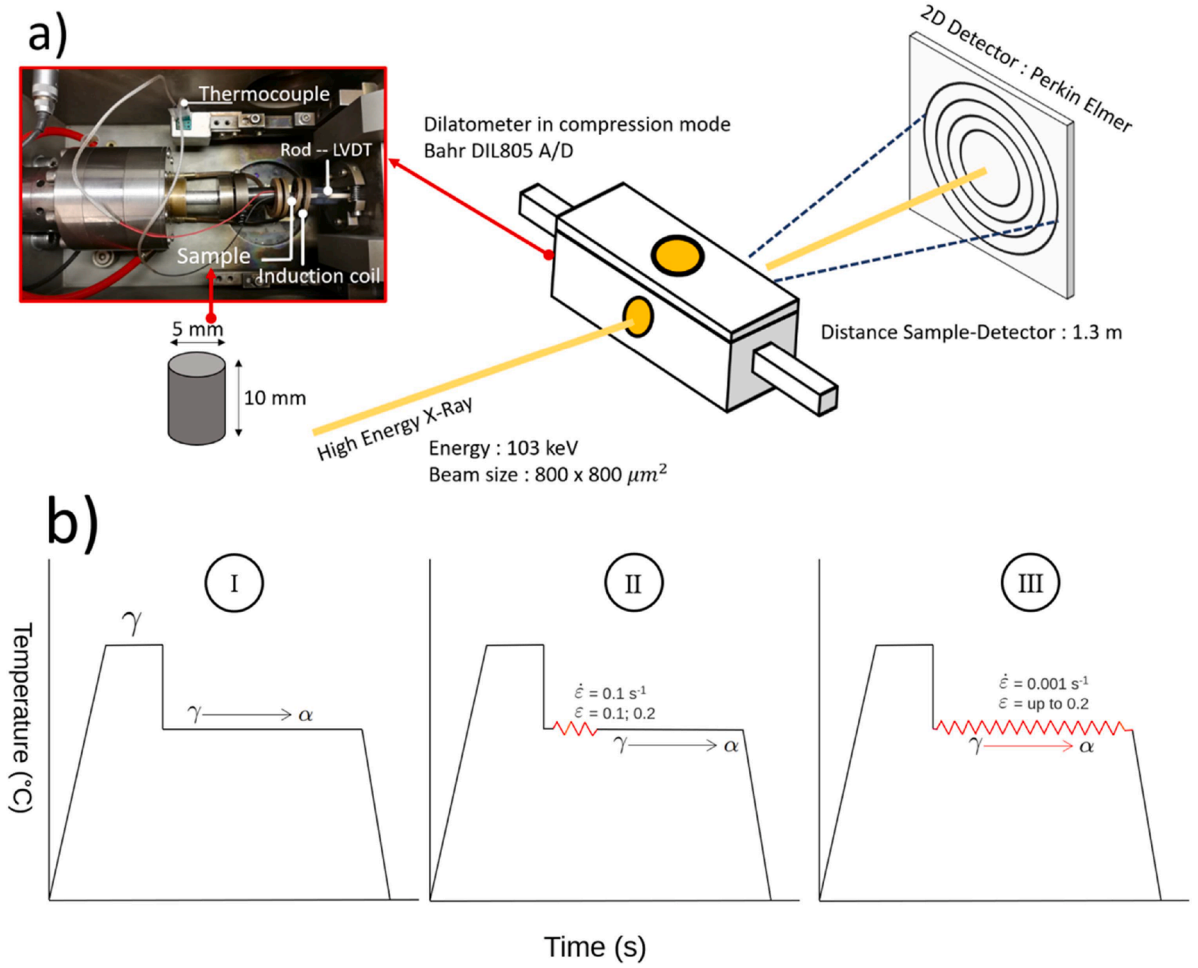

Fig. 1. a) The HEXRD experimental setup showing the position of the furnace, the primary beam and the 2D detector. The upper left side show an image of the 805 DIL Bahr deformation dilatometer used for the experiments with the induction coil, the thermocouple, and the position of the sample. b) Sketch describing the different thermomechanical treatments realized to investigate the effect of deformation on the bainitic transformation: I) deformation-free transformation. II) Ausforming process: $\dot{\varepsilon}$ is the strain rate and ε the applied strain. III) bainitic transformation under deformation.

content in austenite was estimated from the lattice parameter of the FCC phase using the equation reported in [32] :

$$w_C^{\gamma} = w_C^0 + \frac{a_{\gamma} - a_{\gamma_0}(T)}{0.033} \quad (1)$$

where w_C^{γ} and w_C^0 are the mass carbon content in austenite and the bulk content, respectively. a_{γ} is the austenite lattice parameter and $a_{\gamma_0}(T)$ is the reference lattice parameter before bainite starts forming at the isothermal holding temperature, T.

Given that the lattice parameter is affected by both the carbon content and the applied stress, decoupling the two effects is complex. In the ausforming case, the applied stress is removed before the start of the bainitic transformation, and thus the only contributor to the lattice parameter change during the isothermal holding is carbon redistribution. This assumption doesn't hold for the dynamic transformation, and thus only the carbon evolution for the reference case as well as that for the ausformed case are conducted in the present work.

2.3. Microstructural observations

Microstructure observations were carried out using scanning electron microscopy (SEM) and electron backscatter diffraction (EBSD). The samples were cross-sectioned perpendicular to the compression axis and polished using standard metallographic procedures (grinding, polishing, and etching with 2 % Nital). Final polishing of the samples for electron backscatter diffraction (EBSD) was carried out using an OP-U colloidal silica suspension. EBSD measurements were carried out using a JEOL 7000F scanning electron microscope operating at a voltage of 20 kV. The specimens were tilted at an angle of 70 ° and measurements taken at 800× magnification with a step size of 60 nm for an area of 100 μm×100 μm.

Transmission electron microscopy (TEM) was used to investigate carbide formation, both with the direct carbon extraction replica method and by foil analysis. Samples for the extraction replicas were prepared using standard procedures of grinding/polishing to a step of 0.1 μm diamond suspension and coating with a 15–20 nm thick carbon film, upon which precipitates were extracted by immersion in 4 % Nital solution. Thin foils were made by polishing disks to ~80 μm thickness and subsequent jet polishing. Samples were examined with the Thermo Scientific Talos L120C TEM.

3. Results

3.1. Bainitic transformation kinetics

3.1.1. The 400 °C case

Fig. 3-a shows the evolution of bainitic ferrite phase fraction during isothermal holding at 400 °C, as determined by HEXRD experiments, under the three different deformation conditions. When the sample is ausformed, the onset of bainitic transformation is significantly

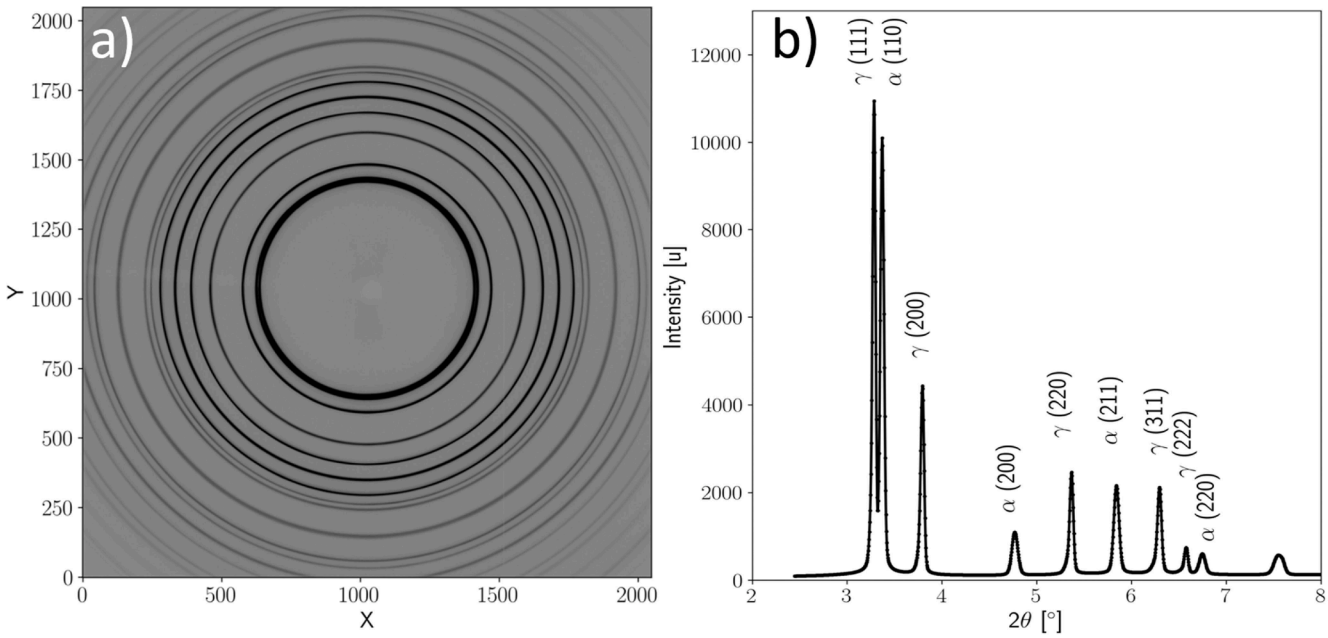

Fig. 2. a) Debey-Scherer rings (or 2D diffraction images) obtained from high energy X-Ray diffraction experiments showing a two phases structure of austenite and ferritic bainite, formed during the isothermal holding. b) Intensity vs. 2θ plots of the integrated 2D image in a), showing the position of different atomic of the two phases (α: bcc-bainitic ferrite and γ: fcc-austenite).

accelerated, compared to the non-deformed sample, but the final fractions reached at the end of the isothermal hold are similar to those without deformation. When the applied ausforming strain is increased from 0.1 to 0.2, the bainitic transformation becomes faster. Using in situ HEXRD measurements, we can confirm that no bainite was formed during the ausforming step. This is shown in Fig. 3-d, where the applied stress during the ausforming process is plotted against time, as well as the ferrite fraction during the ausforming step. The figure indicates that deformation was completed prior to the start of the bainitic transformation, meaning that the deforming phase during the ausforming stage was austenite.

The carbon content in austenite during isothermal holding of both the non-deformed and ausformed samples is shown in Figure S.1 of the supplementary materials. As expected, the increase in ferrite fraction is accompanied with carbon partitioning between austenite and ferrite. The carbon content in austenite progressively increases over time across all samples. The results show an earlier and faster increase in carbon content in austenite for the ausformed samples, with the effect becoming more pronounced at higher ausforming strains.

For the dynamic transformation experiments, the measured kinetics initially follows a similar trend as the non deformed case for times less than 50 s. Subsequently, the measured kinetics gets faster compared to both the ausformed and the non deformed samples, suggesting a clear interaction between the deformation process and the phase transformation. At 400 °C, the bainitic ferrite fraction formed after 100 s of deformation (strain of 0.09) is 77 %, compared to 25 % when no deformation is applied, 56 % when an ausforming strain of 0.1 is applied prior to the transformation, and 66 % when an ausforming strain of 0.2 was used. The abrupt stop of the bainitic ferrite fraction increase is due to the thermocouple detachment from the sample, probably due to the high deformation applied to the sample. As observed in Fig. 3-a, the transformation under deformation stopped after approximately 100 s (corresponding to a strain of 0.09). This interruption was caused by the detachment of the thermocouple from the sample, likely due to the applied strain, which led to the experiment interruption. A similar occurrence was noted at 450 °C (Fig. 3-c), whereas this issue did not arise at 500 °C (Fig. 3-e).

3.1.2. The 450 °C case

The results for the 450 °C case, are shown in Fig. 3-b. Slower kinetics are observed in the non deformed case when compared with the 400 °C. Similar observations are made for the effect of ausforming at 450 °C, where the onset of the bainitic transformation is accelerated when a prior deformation is applied but tends to reach a similar volume fraction at long times as that obtained in the non deformed case. Similarly, no ferrite was formed during the ausforming process, and the transformation started clearly after the ending of ausforming, as shown in Fig. 3-e. Finally, the effect of an applied deformation during the transformation is more pronounced than at 400 °C, where the ferrite fraction after 160 s (i.e., strain of 0.12) reaches 58%, compared to 9% and 22 % for the no deformation sample and the sample that was ausformed to a strain of 0.1, respectively.

3.1.3. The 500 °C case

The evolution of the bainitic ferrite phase fraction during the isothermal holding at 500 °C is shown in Fig. 3-c for the three scenarios of deformation. When no deformation is applied, a very small fraction of bainitic ferrite was formed during the isothermal hold indicating that 500 °C is very close to the bay temperature. No clear effect of ausforming on the kinetics was observed at 500 °C for applied strains of 0.1 and 0.2. Using 0.4 applied strain, a higher bainite fraction is formed during the isothermal hold (9%), however, this ferrite fraction was formed during the ausforming step, as shown in the Fig. 3-f, and thus cannot be considered as ferrite due to ausforming. The 500 °C case is noteworthy, as one can note a much larger fraction of bainitic ferrite formed under dynamic transformation conditions (25%) than the fractions formed in the non-deformed and ausformed cases (< 3 %). Fig. 3-c also shows that after the end of deformation, the ferrite fraction remains constant during the subsequent isothermal hold up to 500 s.

To better visualize the relationship between the applied deformation and the bainitic ferrite growth kinetics during the dynamic transformation, Fig. 4 illustrates the evolution of the bainite volume fraction and the applied stress as a function of the applied strain. During the elastic loading regime, no acceleration of the transformation is observed for the three temperatures. In fact, no bainite is formed during this initial stage. Similarly, at the early stages of plastic deformation of austenite,

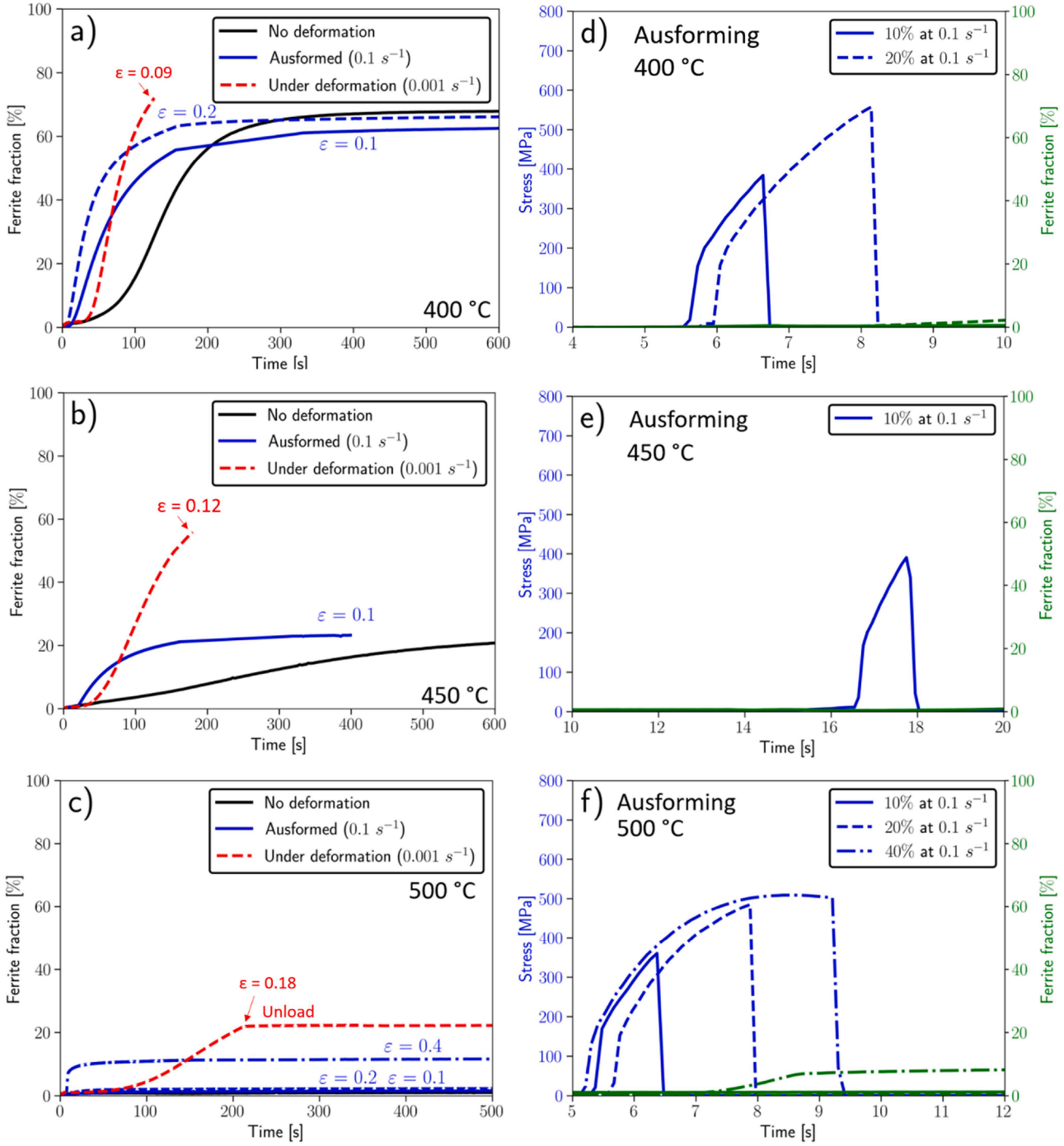

Fig. 3. : a), b) and c) HEXRD measurement of bainitic ferrite fraction evolution during thermo-mechanical processing under various deformation scenarios at different temperatures: a) 400 °C, b) 450 °C, and c) 500 °C. Deformation-free transformation is represented using black lines, ausforming using blue lines, and transformation under deformation using red lines. Figures d), e) and f) show the corresponding stress-strain curves for the ausforming process and the evolution of the ferrite fraction during ausforming step for the corresponding temperatures. The red arrows show the final strain at the end of deformation. No strain was applied beyond this point and the sample was completely unloaded.

no clear effect is noticed on the bainitic transformation. The acceleration of bainite is noticed starting at a plastic strain of ~2 % at 400 °C and 450 °C and starting at a strain of ~5% at 500 °C.

3.2. Post-mortem microstructure

Fig. 5 presents the SEM and EBSD micrographs of the samples obtained after the HEXRD experiments for the 400 °C heat treatment, under the three different deformation conditions. The images show a bainitic microstructure with martensite and retained austenite. Martensite was formed during the final quenching to room temperature. The microstructure of the ausformed sample (Fig. 5-e) has a finer structure and thinner bainite laths compared to the non-deformed sample. It also shows an elongated grain structure due to the applied deformation. When the transformation occurs concurrently with the applied deformation (Fig. 5-f), the microstructure resembles the non-deformed one with a similar grain size and long bainitic ferrite laths that traverse the full grain.

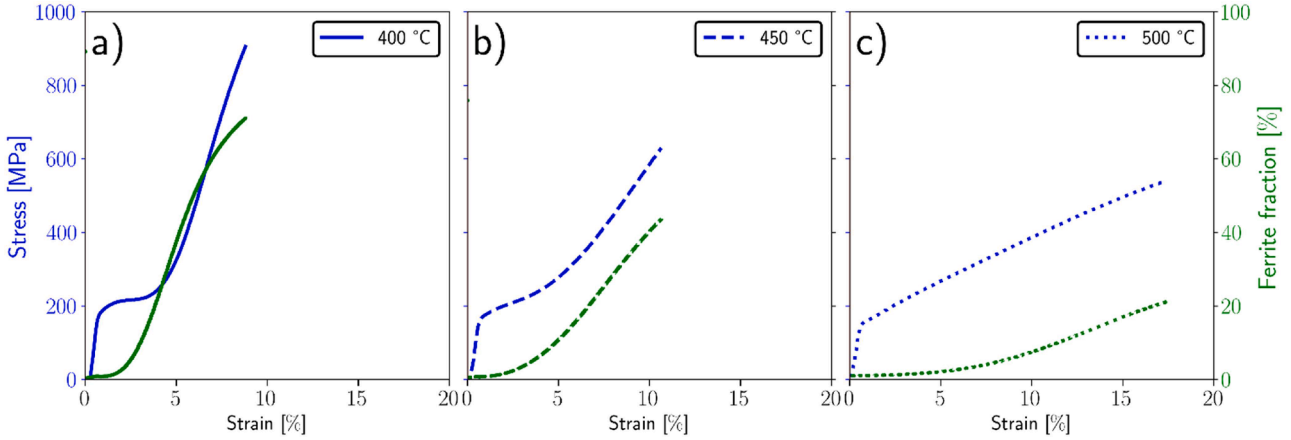

Fig. 4. Evolution of dynamically transformed bainitic ferrite (in green) as a function of the applied strain during the isothermal hold at a) 400 °C, b) 450 °C and c) 500 °C. The evolution of the applied stress during the bainitic transformation is also shown in blue.

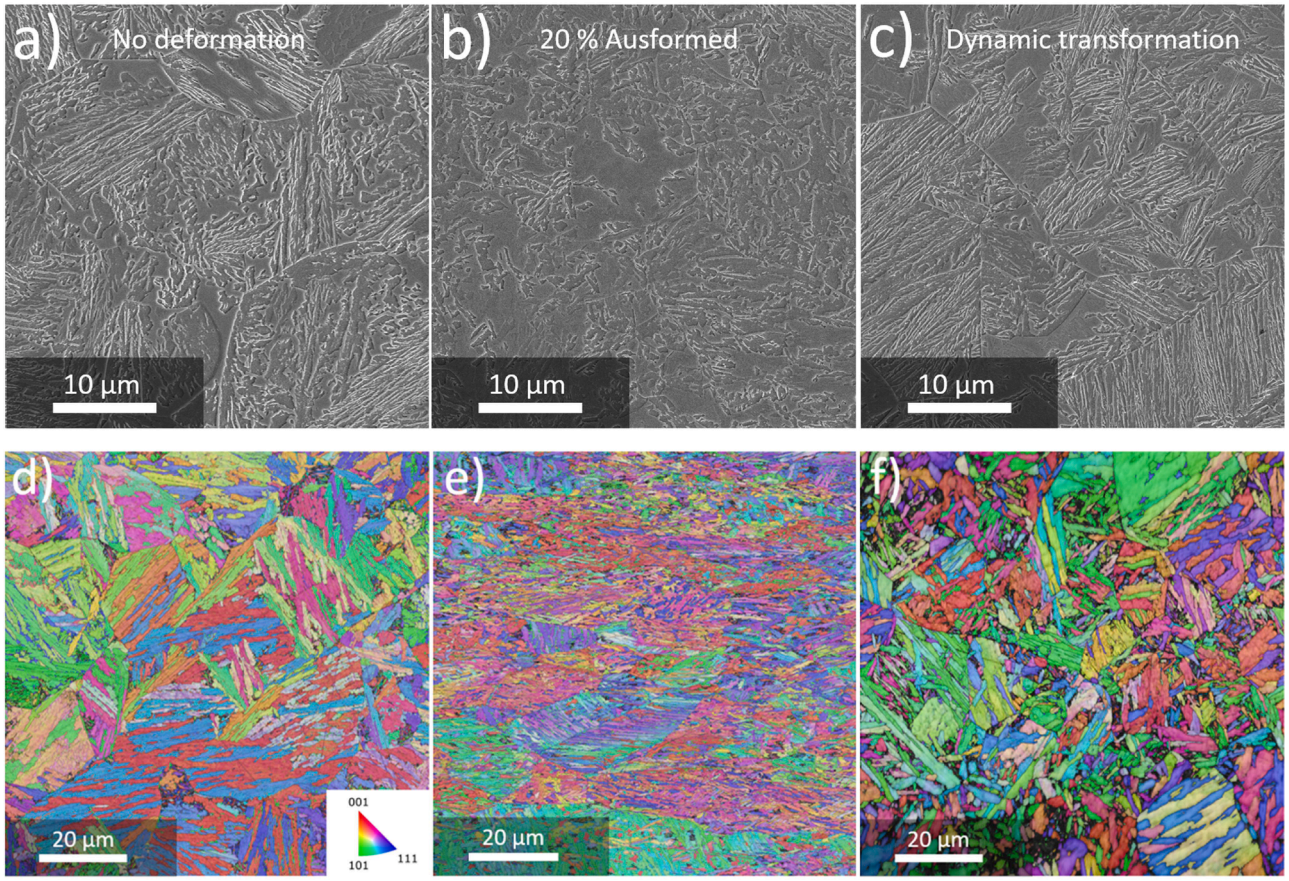

Fig. 5. SEM micrographs (a-c) and EBSD micrographs (d-f) showing the effect of deformation on the resulting microstructure for the sample treated at 400 °C. a) and d) no deformation was applied (pure isothermal transformation), b) and e) sample was ausformed at 20%, c) and f) the sample was deformed up to 10 % during the bainitic transformation.

To investigate the potential effect of carbides on the accelerated kinetics and the high ferrite fractions observed when deformation is applied concurrently with transformation (Fig. 3-a, -c and -d), TEM observations were conducted on two samples treated at 400 °C and 500 °C, both with and without concurrent deformation. At 400 °C, results indicated that no or very limited carbides formed during the experiment in both cases (Fig. 6-a and -b). However, at 500 °C, no carbides were detected in the reference sample, in contrast to the deformed sample, where clear carbide precipitation was observed in Fig. 6-d and confirmed by the selected area diffraction (SAD) pattern shown in Fig. 6-e.

4. Discussion

4.1. *Effect of ausforming*

The above experiments showed that the bainitic transformation was initially accelerated by the ausforming process as compared to the

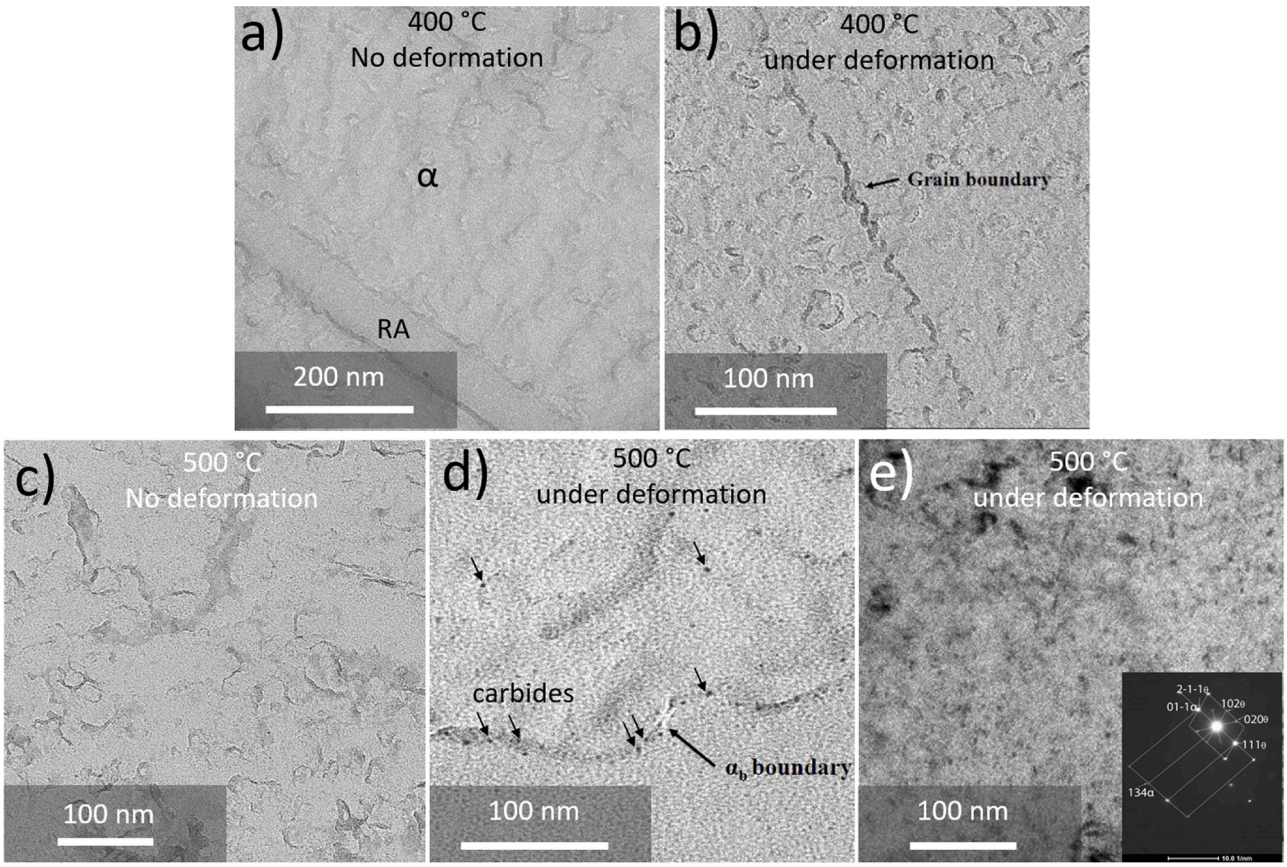

Fig. 6. TEM image for the samples treated isothermally at 400 °C (a and b) and at 500 °C (c, d and e). a) and c): without deformation. b), d) TEM images for the sample dynamically deformed at 500 °C, showing the presence of carbides at the bainite boundaries. e) Thin foil TEM micrograph and its corresponding SAD (selected area diffraction) pattern confirming the carbide structure for the same sample shown in d).

transformation that took place without deformation. However, as time progressed, the transformation slowed down and eventually reached similar bainite fractions to those observed in experiments where no deformation was present. This study covered a limited range of deformation conditions, specifically, tensile deformation up to strains of 0.2 and strain-rates of up to 0.1 s^{-1}. The discussion is, therefore, limited to these conditions. It is possible that other interactions between deformation and bainite formation take place under different deformation conditions [4,27].

Similar observations have been reported in the literature, suggesting a two-stage transformation kinetics characterized by a fast rate of transformation at the beginning and a slower rate at later stages [4,14,16]. The initial acceleration due to ausforming has previously been attributed to an enhanced nucleation rate, caused by the high-density of defects in the deformed austenite [14,15]. On the other hand, the interface movement can be hindered by the structural defects present in the deformed matrix, e.g., forest dislocation. This slows down the growth of bainitic ferrite laths [14,16,17]. The overall growth rate ultimately depends on the balance between these two opposing mechanisms. The initial fast increase in the measured bainitic ferrite in the ausformed samples indicates an acceleration of the nucleation rate. The accelerated nucleation due to ausforming is also supported by the present microstructural observations. Fig. 5-b ande, clearly show the finer microstructure of the ausformed samples compared to the non deformed case. This indicates a higher number of nuclei, followed by limited growth, both as a result of the high density of dislocation which were created during prior deformation [15,16,33].

4.2. *Effect of dynamic deformation*

When deformation is applied during the formation of bainitic ferrite, the outcome is quite different. The transformation rate increases with an increase in the applied deformation, and the amount of bainitic ferrite produced is larger compared to both the deformation-free and ausformed cases. The acceleration of bainite formation with concurrent deformation has been established in previous studies [6,11,34,35], but the underlying cause of this phenomenon remains unclear. The acceleration of the transformation kinetics can be attributed to either an increase in the nucleation sites introduced by the continuous plastic deformation [21] or to an additional mechanical driving force for the transformation introduced by the applied stress [36]. A third possibility is that differences in carbide precipitation kinetics impact the transformation.

While the nucleation step is clearly accelerated in the ausformed case (as shown by both kinetics in Fig. 3 and the postmortem microstructural observations), nucleation does not seem to be affected when the deformation is applied concurrently during the transformation as shown by the kinetics in Fig. 3. Microstructural observations support this conclusion. An increase in nucleation would result in a finer microstructure; however, the micrographs in Fig. 5 indicate that the microstructure in the specimen subjected to concurrent deformation (Fig. 5-f) is similar to that of the deformation-free specimen (Fig. 5-d). However, the bainitic ferrite fraction formed under dynamic transformation is significantly higher than that formed under ausforming conditions, suggesting that the growth rate during the dynamic transformation is much higher than during the ausforming process. The present results are therefore more consistent with the second theory that the applied deformation increases the lengthening rate of bainitic ferrite by increasing the transformation

driving force through an additional mechanical energy.

However, it could be argued that the absence of the effect of concurrent deformation on nucleation is due to the low strain rate used in this study ($10^{-3}\ s^{-1}$), and that increasing the strain rate may accelerate the nucleation rate accordingly. Further investigations are, therefore, needed to thoroughly explore the effect of strain rate on the transformation kinetics of bainite. For instance, Zaymovskiy et al. [27] demonstrated that increasing the strain rate accelerates the bainitic transformation. However, no distinction has been made regarding the strain rate's effect on the nucleation versus the growth process.

4.3. The possible effect of carbides

The potential role of carbide formation in accelerating bainitic growth and contributing to the high bainite fraction at the end of isothermal holding, particularly evident at 500 °C, deserves attention. Carbide formation can be ruled out at 400 °C due to the sluggish nature of carbide precipitation at this temperature (confirmed by TEM observations shown in Fig. 6-a and Fig. 6-b). Moreover, the comparable final bainitic ferrite fractions at 400 °C across all samples indicate a similar carbon sink in both cases.

A notable finding of this study is the observed effect of deformation on transformation kinetics at 500 °C. It appears that the bainite start (Bs) temperature may differ under dynamic transformation conditions compared to non-deformed and ausformed scenarios. This is evident from the absence of ferrite in the non-deformed and ausformed samples at 500 °C, suggesting a Bs temperature above 500 °C. Conversely, clear observation of bainitic ferrite under dynamic conditions implies that, in this scenario, the Bs temperature is higher than 500 °C. Eres-Castellanos et al. [1,37] reported an increase in the bainite start temperature when stresses were applied during the transformation. They estimated the shift in the bainitic start temperature under applied deformation by incorporating mechanical energy into the driving force for bainite nucleation [1]. Their findings concluded that this additional driving force could shift the transformation temperature to higher values, as supported by their experimental observations.

The accelerated kinetics under dynamic transformation conditions at 500 °C cannot be attributed to a nucleation acceleration, as can be seen from Fig. 3. If the role of deformation were to induce additional nucleation sites, a pronounced increase in ferrite fraction in the ausformed sample would have been expected. Given the low ferrite content in the ausformed sample, it is more plausible that the ferrite formation under dynamic conditions at 500 °C is linked to an increased growth rate. This increase in growth rate may result from either the mechanical energy term or a dynamic precipitation of carbides, offering an extra carbon sink.

To explore the latter hypothesis, transmission electron microscopy (TEM) observations were conducted on the same samples used for HEXRD at 500 °C (Fig. 5), both under non-deformed and dynamically deformed conditions. Carbides were visibly present when dynamic deformation was applied (Fig. 6-b and -c), while the non-deformed case exhibited very limited carbide presence. This indicates that the increased ferrite fraction at 500 °C is partially attributed to carbide precipitation. To quantify this effect, TEM images could be used to estimate the carbon content present in carbides versus that retained in austenite. Similar calculations were conducted by Quidort et al. [38] to understand the effect of carbides on bainite growth kinetics. Although these calculations are approximate, they suggest a comparable carbon flux toward carbides and into austenite in the non-deformed case. To quantify this effect in the present case, the carbon rejected from the bainitic ferrite can be estimated from HEXRD results. The carbon mass balance can be written as follows:

$$x_C = f^{\alpha}x_C^{\alpha} + f^{\gamma}x_C^{\gamma} + f^{\theta}x_C^{\theta} \tag{2}$$

where x_C is the nominal carbon content of the alloy, x_C^i is the carbon content in ferrite (α), austenite (γ) and cementite (θ) and f^i is the phase volume fraction. The ferrite fraction is estimated from HEXRD at the end of the transformation. Based on Fig. 3-c, the volume fraction of bainitic ferrite is 24 %. The carbon content in ferrite and cementite can be estimated using ThermoCalc [39], considering equilibrium conditions at 500 °C. While the equilibrium hypothesis for bainite can be debated [40–42], it is likely that at these relatively high temperature, bainite does not exhibit significant carbon supersaturation [41,43]. Furthermore, this analysis only considered cementite carbides and did not account for transition carbides. The carbon content in austenite is estimated from the lattice parameter using Eq. (1). The calculations show that only 20 % of the rejected carbon ended up in the formed carbides. This clearly shows that carbides are not solely responsible for the observed ferrite; rather, deformation also has a significant impact. This reinforces the notion that mechanical forces have played a role in increasing the growth of bainitic ferrite under dynamic deformation conditions.

The current observations highlight that ausforming has the most significant effect on nucleation at temperatures below 500 °C. The growth of bainitic ferrite plates rapidly slows in ausformed samples, whereas under dynamic deformation conditions, there is a notable enhancement in bainitic ferrite growth. Although carbide precipitation was observed at 500 °C, its effect on the overall kinetics is not sufficient to explain the present findings. In Section 4.4 we rationalize the experimental observations by proposing a modified Zener-Hillert model that incorporates the effect of applied deformation.

4.4. Modelling the effect of deformation on plate-like ferrite growth kinetics

In a previous contribution [28], the authors have developed a new model to describe the lengthening kinetics of bainitic ferrite laths. This model will now be extended to examine the impact of deformation on the lengthening kinetics of plate-like ferrite. The model assumes that the growth of bainite is controlled by the diffusion of carbon in austenite. The Zener-Hillert formulation is used to define the maximum velocity of the interface, v_{max}.

$$v_{max} = \frac{D}{L}\frac{x^{\gamma/\alpha} - x^0}{x^0 - x^{\alpha/\gamma}} \tag{3}$$

The carbon mole fractions x^0, $x^{\gamma/\alpha}$, and $x^{\alpha/\gamma}$ are, respectively, the carbon mole fraction in the bulk, the carbon mole fraction at the austenite side of the interface, and the carbon mole fraction at the ferrite side of the interface. The carbon diffusion coefficient in austenite is represented by D. The diffusion distance, L, is proportional to the radius of curvature of the growing needle, r and expressed as $L = ar$, where a was estimated by Hillert [44] to be 2. To determine the interface conditions ($x^{\gamma/\alpha}$ and $x^{\alpha/\gamma}$), the authors employed a local energy balance at the interface.

$$\Delta G_m^{chem} = \Delta G_m^{diss} + \Delta G_m^{fric} + \Delta G_m^{r} + \Delta G_m^{mec} \tag{4}$$

The energy balance at the interface was calculated using the following components:

- ΔG_m^{chem}, which represents the chemical driving force for growth. It was calculated using the expression proposed by Hutchinson et al. [45]:

$$\Delta G_m^{chem} = \sum^{X}\left\{\frac{\left(u_X^{\alpha} + u_X^{\gamma}\right)}{2}\left(\mu_X^{\gamma,i} - \mu_X^{\alpha,i}\right)\right\} + \frac{\left(u_{Fe}^{\alpha} + u_{Fe}^{\gamma}\right)}{2}\left(\mu_{Fe}^{\gamma,i} - \mu_{Fe}^{\alpha,i}\right) \tag{5}$$

The mole fractions of Fe and X in the substitutional matrix are represented by $u_{Fe} = \frac{x_{Fe}}{1-x_C}$, and $u_X = \frac{x_X}{1-x_C}$, respectively, while μ is used to

denote the chemical potential.

- ΔG_m^{diss} and ΔG_m^{fric}, represent, respectively, the dissipated energy due to solute drag and interface friction. Both were assumed to be negligible at the temperatures considered in this work.
- ΔG_m^r, represents the curvature energy and was expressed as: $\Delta G_m^r = V_m \frac{\sigma^{\gamma/\alpha}}{r}$, where V_m is the molar volume of ferrite and $\sigma^{\gamma/\alpha}$ is the interfacial energy.

Para-equilibrium was used as the starting state of the transformation. The thermodynamic parameters were determined using the TCFE9 database of ThermoCalc [39].

The new aspect of this model [27] was the introduction of a mechanical energy term, ΔG_m^{mec}, which is based on the interaction between the moving interface and the existing defects in the austenite matrix. This energy was described using the equation:

$$\Delta G_m^{mec} = \widehat{\sigma}\frac{b}{\Lambda}m_s \tag{6}$$

where $\widehat{\sigma}$ (the internal back stress) represents the opposing force generated by the defects (such as dislocations and solute elements), m_s is the Schmid factor, b is the magnitude of the Burgers vector, and Λ is the mean free distance of a mobile disconnection.

In the present contribution, Eq. (6) will be modified to incorporate the effect of deformation in the following way:

$$\Delta G_m^{mec} = (\widehat{\sigma} - \sigma)\frac{b}{\Lambda}m_s \tag{7}$$

In this formulation, the mechanical energy is described using two parameters: (1) the internal back stress $\widehat{\sigma}$, which represents the opposing force to the movement of the interface, and (2) the austenite flow stress σ, which represents the effect of an external stress applied during the transformation and can be regarded as a driving force for the transformation as will be explained subsequently.

The internal back stress, $\widehat{\sigma}$, arises from the interaction between the interface and existing dislocations and solute atoms in the matrix near the moving interface [46,47]:

$$\widehat{\sigma} = \alpha M \mu b\sqrt{\rho} + \sigma_{SS} \tag{8}$$

where M is the Taylor factor, μ is the shear modulus, α is a constant value of the order of 0.15 for austenite and ρ is the dislocation density in the matrix. The solid solution hardening, σ_{SS}, contribution is calculated as [28]:

$$\sigma_{SS} = 15.4(5.7 + 23w_C + 0.24w_{Cr} + 0.94w_{Mo} + 1.3w_{Si} + 0.123w_{Mn} + 0.012w_{Ni}) \times \left(1 - 0.26 \times 10^{-2}T_C + 0.47 \times 10^{-5}T_C^2 - 0.326 \times 10^{-8}T_C^3\right) \tag{9}$$

It is evident that the mechanical energy term (Eq. (7)) is a function of both the applied stress and the resulting internal back stress. The two stresses are related by the kinetic equation that links the flow stress (σ) to the strain rate ($\dot{\epsilon}$) [46]:

$$\frac{\sigma}{\widehat{\sigma}} = \left(\frac{\dot{\epsilon}}{\dot{\epsilon_0}}\right)^{\frac{1}{m}} \tag{10}$$

where $m = \frac{\partial \ln\sigma}{\partial \ln\dot{\epsilon}}$ is the strain rate sensitivity parameter and $\dot{\epsilon_0}$ is a material property set here to 5.10^{-8}.

These two components of mechanical energy (σ and $\widehat{\sigma}$) have parallels in other studies. Patel and Cohen [48] introduced a mechanical driving energy for martensitic transformation, characterized by both shearing and dilatation strains. Conversely, Chatterjee et al. [17] described a mechanical opposing force for bainitic transformation, defined as the force required for dislocations to move past each other.

4.4.1. Effect of ausforming

The model described above can be used to explain the effect of deformation on the growth kinetics of bainite.

In the case of ausforming, where austenite is deformed prior to the transformation, the dislocation density in the matrix increases, resulting in an increase in the internal back stress $\widehat{\sigma}$, as described by Eq. (8). During the transformation, no stress is applied, and the applied stress σ is assumed to be zero. Therefore, the mechanical energy term described by Eq. (7) acts solely as an opposing force to the phase transformation. To illustrate this effect, the model is used to calculate the evolution of the maximum lengthening velocity of bainitic ferrite as a function of the prior deformation strain at different temperatures (400 °C, 450 °C and 500 °C). The stress-strain curves during the compression experiments are shown in Fig. 7-a and the dislocation density in the deformed structure for a given applied stress is estimated using Eq. (11):

$$\rho = \left[\frac{(\sigma - \sigma_0)}{\alpha M \mu(T) b}\right]^2 \tag{11}$$

where σ is the flow stress at the end of the ausforming process and σ_0 is the initial yield strength, extracted from Fig. 7-a. The internal back stress at the transformation temperature is calculated using Eq. (8) and the corresponding mechanical energy is calculated using Eq. (7).

The calculations showing the evolution of the maximum plate lengthening velocity as a function of the ausforming strain is shown in Fig. 7-b for the three temperatures of interest. The model predicts that the maximum lengthening velocity of the bainitic ferrite needles decreases with increasing prior deformation strain. This is to be expected since the plastic deformation increases the dislocation density in the matrix and thus increases the opposing mechanical energy term (Eq. (6)). The underlying mechanism is that the forest dislocations hinder the movement of the interface during growth. This is a natural consequence of the interaction of interfacial disconnections with the defects present in the matrix. Hu et al. [49] described a second possible effect of prior deformation on lengthening kinetics. They argued that as the bainitic ferrite plate advances into the misorientation gradients that prior deformation created in austenite, the OR between the plates and the matrix deviates from the ideal K-S orientation and this further slows down the transformation. This mechanism could also be incorporated into the present model by developing an expression for the change of the spacing of disconnections due to the change of the orientation of the austenite. Given that our experimental data does not provide measurements of the lengthening rates of individual plates, we did not attempt to incorporate this possible second effect.

4.4.2. Effect of deformation during the bainitic transformation

Next the lengthening kinetics of bainitic ferrite formed concurrently during deformation is considered. The challenge here is to calculate the internal back stress during deformation to estimate the mechanical energy term. A solution is to use the kinetic Eq. (10). To this end, the value of m was determined through strain-jump experiments on the present steel. The stress-strain curves obtained at two temperatures, 825 °C and 900 °C, and using two strain rates, 1 s^{-1} and 0.1 s^{-1}, are shown in Fig. 8-a. These temperatures were selected to avoid any deformation induced

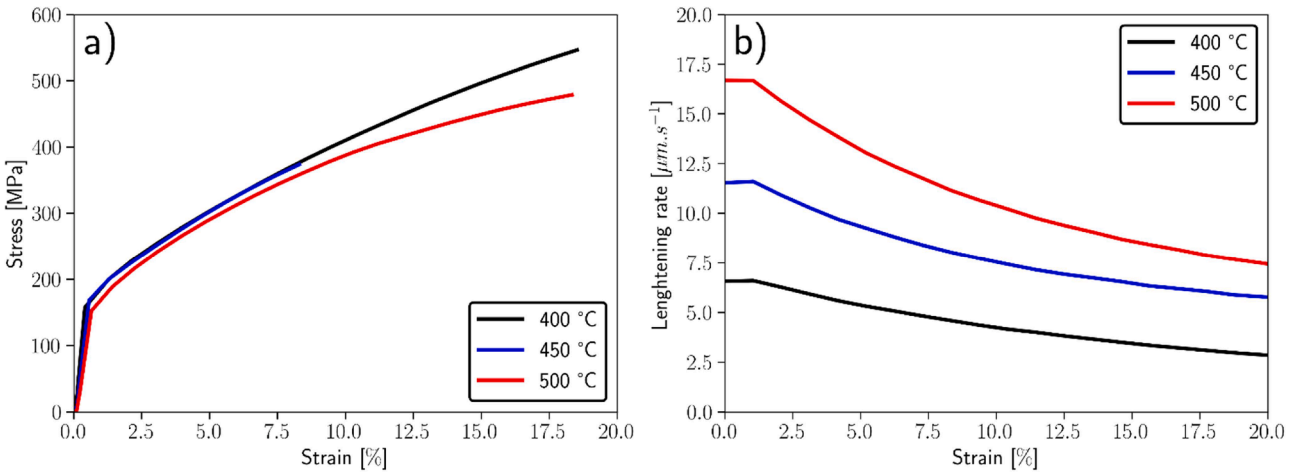

Fig. 7. a) Stress-strain curves during the ausforming process at the three temperatures, 400 °C, 450 °C and 500 °C, respectively. b) the evolution of bainite growth rate as a function of the applied stress during the ausforming process, as calculated by the present model.

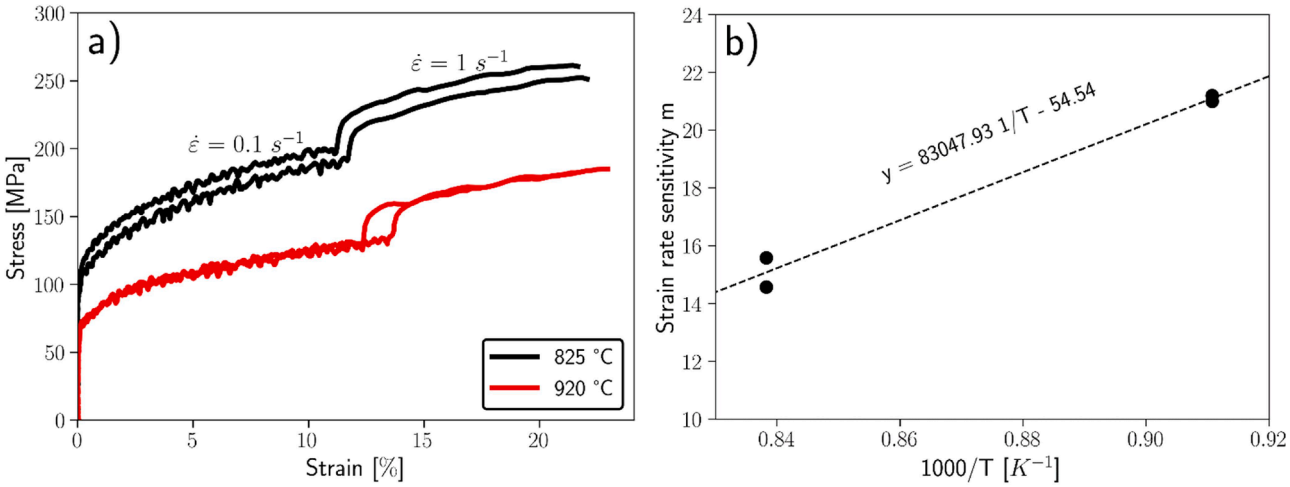

Fig. 8. a) Stress-strain curves showing the strain rate jump experiments performed at two strain rates, 0.1 s^{-1} and 1 s^{-1} and at two temperatures 825 °C and 900 °C, to evaluate the strain rate sensitivity parameter m. b) The obtained values of (m) as a function of temperature.

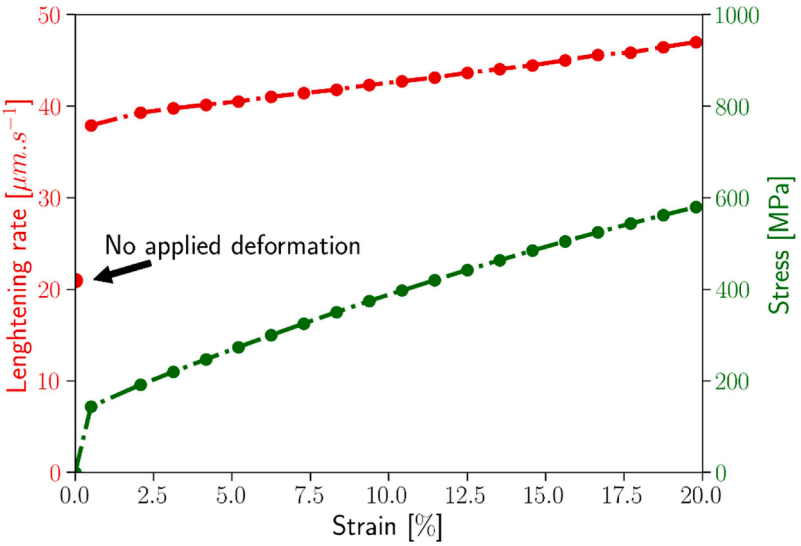

Fig. 9. The calculated plate-like lengthening rates as a function of the applied deformation at 500 °C in red. Figure also shows the evolution of the applied stress during the transformation in green.

phase transformations in austenite. The rate sensitivity parameter m obtained at the two temperatures is shown in Fig. 8-b. Using a linear fit, the rate sensitivity parameter was estimated by extrapolation to the temperature range of our experiments.

The applied stress was then obtained directly from the stress-strain curves and the internal back stress was calculated from Eq. (10), allowing us to calculate the mechanical energy term (Eq. (7)). The model was then used to calculate the lengthening rate of bainitic ferrite plates. The lengthening rate at 500 °C, is shown in Fig. 9. The model suggests that even a small, applied strain can accelerate the lengthening rate of bainitic ferrite plates and that the acceleration exhibits a linear relationship with the increase in applied strain. This is consistent with both the current observations and previously reports in the literature [6,36]. According to our model, the acceleration of the transformation is due to the increase of the driving force generated by the applied stress. Additionally, the acceleration of the bainitic transformation is only effective while a strain is applied, meaning that once the deformation stops, the acceleration of plate lengthening stops as well. This observation is consistent with the behaviour observed at 500 °C (Fig. 3-c), where the ferrite fraction stopped increasing at the same time the deformation was stopped. The model captures this by introducing a mechanical driving force which is proportional to $(\sigma - \widehat{\sigma})$.

The present findings indicating that the transformation stops as soon as the applied deformation is stopped, may suggest that the transformation is strain driven. However, several studies have shown an acceleration of the bainitic transformation under a constant applied stress, indicating that the transformation is also stress driven. For instance, Bhadeshia et al. [50] and Shipway et al. [6] reported that even a constant elastic deformation accelerates the transformation rate of bainitic transformation. One should note that in the reported studies, the applied stress was in the elastic regime of austenite, while the present study applied a plastic deformation. Other studies reported that an acceleration of the transformation under applied constant stress higher than yield stress of the austenite [35,37,51]. However, those studies didn't report if the observed acceleration is due to a nucleation effect or a growth effect. Another study by Liu et al. [11] investigated the effect of an applied constant stress once the bainitic transformation attained the plateau. The results clearly showed that the applied stress didn't have any effect on the kinetics. Clearly, more work should be carried out to clarify this aspect.

Unlike ausforming, an imposed deformation during the transformation increases the driving force for the transformation. To show the difference between the two scenarios, Fig. 10 represents the magnitude of the mechanical energy term as a function of the applied stress for the two cases at 500 °C. In the absence of any applied deformation, the mechanical energy term is solely due to defects in the matrix (i.e., dislocations and solute atoms). This results in a barrier energy of around +200 J.mol^{-1} as shown in Fig. 10. During ausforming, the magnitude of the barrier energy increases with increasing applied strain, due to the multiplication of dislocations during plastic deformation. As the barrier increases, the movement of the interface is retarded, and the lengthening rate decreases as a result. However, when deformation is applied during the bainitic transformation, the mechanical energy term includes the applied stress. For a positive strain rate, the applied stress is greater than the back stress and as a result the value of the mechanical term becomes negative, indicating that it is now acting as a driving energy that accelerates the transformation. The magnitude of the mechanical driving force also increases with the applied strain.

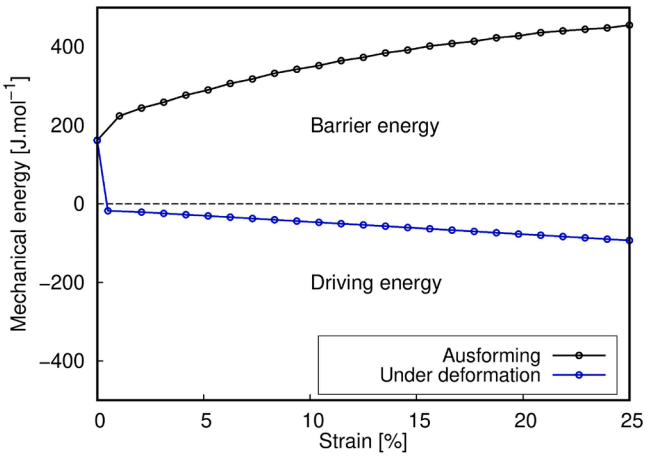

Fig. 10. The evolution of the mechanical energy as a function of the applied strain in the two deformation scenarios: ausforming (black) and under deformation (blue). The positive values of the mechanical energy are considered as a barrier energy for the transformation and negative values as a driving energy.

One aspect that should be discussed in the present work is the effect of elastic deformation on bainite growth kinetics. Elastic deformation does not impact the defects structure in the matrix; hence, it should not affect the barrier term $(\widehat{\sigma})$. However, applied elastic deformation can accelerate the transformation through the driving term (σ) in the Eq. (7). Consequently, the resolved shear stress acting on the disconnection can accelerate the transformation. The detector framerate used in this study did not provide sufficient insight into the transformation behavior under elastic deformation conditions. However, previous studies have shown that elastic deformation accelerates the overall transformation of bainite [5,37,50,52].

4.5. Limitations and future work

The present model captures the effect of deformation on the diffusional growth of plate shaped ferritic products. The mechanical energy term introduced in this work is based on the interaction between stress and the disconnections at the tip of the plate. For this reason, this approach only applies to diffusional- displacive transformations. It would not apply to reconstructive transformations for which the movement of the interface does not involve the movement of disconnections. Consequently, the mechanical energy term introduced here could not be used to describe the effect of deformation on the growth of allotriomorphic ferrite regardless of the OR between the ferrite grains and the austenite matrix.

The present study helped identify the effect of ausforming and concurrent deformation on the bainitic transformation. However, some limitations of the reported observations must be clearly stated. First, the reported observations have been obtained for a limited range of strain and strain rates. For instance, for the ausforming test, the maximum applied strain was 0.2 and the maximum strain rate was 0.1 s^{-1}. It was reported in other studies that applying a larger strain during ausforming results in a higher stabilization of austenite, and thus, a lower bainitic ferrite fraction formed at the end of the isothermal holding [1,4]. The present study showed that the obtained bainite fraction was always comparable to the non-deformed case, independent of the strain applied up to 0.2. Similarly, the kinetics may be impacted by the strain rate [27] and as such, the present conclusions are limited to the strain-rates that were investigated in this study. Similar comments can be made for the case in which the phase transformation occurred while the specimen is being deformed. Therefore, readers should keep in mind that the behavior observed here cannot necessarily be generalized to deformation conditions outside of those studied in our experiments. Future studies are needed to clarify the effect of deformation on the bainitic transformation for a wide range of deformation conditions.

Another aspect that was not deeply discussed in the present work is the effect of elastic deformation on the bainitic transformation. Indeed, the acquisition rate didn't allow us to collect sufficient data prior to the yielding of the specimens. Exiting literature [6,37,50,52], however, suggests that elastic deformation can enhance the transformation rate. The present model predicts such a behavior, as discussed above. Experimental validation, however, will require additional experiments

that focus specifically on the elastic deformation range.

In order to develop the present model into a predictive quantitative model a number of additions are needed. The first is a robust constitutive model for the deformation of austenite to calculate σ and $\hat{\sigma}$ in the mechanical energy term. It is also necessary to obtain accurate data for the lengthening of bainitic ferrite plates under various deformation conditions. Such data could be obtained using confocal laser scanning microscopy. This data would be essential for tuning the model and ensuring its accuracy.

Finally, it is important to point out that the present model only describes the lengthening kinetics of bainitic ferrite plates. To predict the overall transformation kinetics, it will be necessary to develop nucleation models that capture the effect of deformation.

5. Conclusions

HEXRD measurements and microstructure observations demonstrate that:

- Ausforming increases the initial transformation rate of bainite due to an increase in nucleation rate. The bainite growth rate is reduced by prior deformation. The final fraction of bainite in the ausformed sample is similar to that obtained in the non-deformed material.
- Deformation during the bainite transformation increases the transformation rate as already reported in the literature. Under the present deformation conditions, this increase has been shown to be primarily due to an accelerated growth rate, with minimal impact on the nucleation process. Additionally, it was observed that deformation increases the final fraction of bainite.
- Although carbides play a role in inducing the high ferrite fraction observed at 500 °C, the primary factor accelerating the transformation under deformation is the additional mechanical energy introduced by the applied deformation.

A modeling framework has been developed to describe the effect of deformation on the lengthening kinetics of bainitic ferrite plates. Based on the model, the effect of deformation on the transformation kinetics can be rationalized as follows:

- Deformation prior to the onset of the bainitic transformation (ausforming) increases the dislocation density in the matrix, generating an opposing force for the movement of the interfacial disconnections. The growth kinetics is thus decreased.
- An applied deformation during the transformation, can create a driving force for moving the interfacial disconnections. This can increase the maximum lengthening rate of bainitic ferrite plates.

CRediT authorship contribution statement

Imed-Eddine Benrabah: Writing – review & editing, Writing – original draft, Methodology, Investigation, Formal analysis, Conceptualization. **Arina Deboer:** Writing – review & editing, Methodology, Formal analysis. **Guillaume Geandier:** Writing – review & editing, Methodology, Data curation. **Hugo Van Landeghem:** Writing – review & editing, Methodology, Conceptualization. **Christopher Hutchinson:** Writing – review & editing, Formal analysis, Conceptualization. **Yves Brechet:** Writing – review & editing, Formal analysis, Conceptualization. **Hatem Zurob:** Writing – review & editing, Supervision, Resources, Funding acquisition, Formal analysis, Conceptualization.

Declaration of competing interest

The authors declare that they have no known competing financial interests or personal relationships that could have appeared to influence the work reported in this paper.

Acknowledgments

We acknowledge DESY (Hamburg, Germany), a member of the Helmholtz Association HGF, for generously providing us with experimental facilities. We also extend our appreciation to Dr. N. Schell and Dr. A. Stark for their assistance in using beamline P07 at PETRA III. HZ acknowledges the support of the Natural Science and Engineering Research Council of Canada. The authors are grateful to JD Embury for valuable discussions. Support of technical staff at the Canadian Center for Electron Microscopy (CCEM) at McMaster University is acknowledged. Lastly, the CannmetMATERIALS is acknowledged for providing the steel alloy for the study.

Supplementary materials

Supplementary material associated with this article can be found, in the online version, at doi:10.1016/j.actamat.2024.120195.

References

[1] A. Eres-Castellanos, F.G. Caballero, C. Garcia-Mateo, Stress or strain induced martensitic and bainitic transformations during ausforming processes, Acta Mater 189 (2020) 60–72, https://doi.org/10.1016/j.actamat.2020.03.002.
[2] H. Fan, A. Zhao, Q. Li, H. Guo, J. He, Effects of ausforming strain on bainite transformation in nanostructured bainite steel, Int. J. Miner. Metall. Mater. 24 (2017) 264–270, https://doi.org/10.1007/s12613-017-1404-7.
[3] D.N. Hanlon, J. Sietsma, S. van der Zwaag, The Effect of Plastic Deformation of Austenite on the Kinetics of Subsequent Ferrite Formation, ISIJ Int 41 (2001) 1028–1036, https://doi.org/10.2355/isijinternational.41.1028.
[4] H. Hu, H.S. Zurob, G. Xu, D. Embury, G.R. Purdy, New insights to the effects of ausforming on the bainitic transformation, Mater. Sci. Eng. A 626 (2015) 34–40, https://doi.org/10.1016/j.msea.2014.12.043.
[5] P.H. Shipway, H.K.D.H. Bhadeshia, Mechanical stabilisation of bainite, Mater. Sci. Technol. 11 (1995) 1116–1128, https://doi.org/10.1179/mst.1995.11.11.1116.
[6] P.H. Shipway, H.K.D.H. Bhadeshia, The effect of small stresses on the kinetics of the bainite transformation, Mater. Sci. Eng. A 201 (1995) 143–149, https://doi.org/10.1016/0921-5093(95)09769-4.
[7] H. Hu, G. Xu, L. Wang, M. Zhou, Z. Xue, Effect of ausforming on the stability of retained austenite in a C-Mn-Si bainitic steel, Met. Mater. Int. 21 (2015) 929–935, https://doi.org/10.1007/s12540-015-5156-5.
[8] A. Shibata, Y. Takeda, N. Park, L. Zhao, S. Harjo, T. Kawasaki, W. Gong, N. Tsuji, Nature of dynamic ferrite transformation revealed by in-situ neutron diffraction analysis during thermomechanical processing, Scr. Mater. 165 (2019) 44–49, https://doi.org/10.1016/j.scriptamat.2019.02.017.
[9] J.-K. Choi, D.-H. Seo, J.-S. Lee, K.-K. Um, W.-Y. Choo, Formation of Ultrafine Ferrite by Strain-induced Dynamic Transformation in Plain Low Carbon Steel, ISIJ Int 43 (2003) 746–754, https://doi.org/10.2355/isijinternational.43.746.
[10] Y. JR, H. CY, H. WH, Mechanical stabilization of austenite against bainitic reaction in Fe–Mn–Si–C bainitic steel, Mater. Trans. JIM 37 (1996) 579–585.
[11] M. Liu, G. Xu, J. Tian, Q. Yuan, M. Zhou, H. Hu, The Effect of Stress on Bainite Transformation, Microstructure, and Properties of a Low-Carbon Bainitic Steel, Steel Res. Int. 90 (2019) 1900159, https://doi.org/10.1002/srin.201900159.
[12] F.G. Caballero, H.K.D.H. Bhadeshia, K.J.A. Mawella, D.G. Jones, P. Brown, Very strong low temperature bainite, Mater. Sci. Technol. 18 (2002) 279–284, https://doi.org/10.1179/026708301225000725.
[13] A. Eres-Castellanos, Effect of ausforming on the bainitic transformation in medium carbon steels, (n.d.).
[14] S.B. Singh, H.K.D.H. Bhadeshia, Quantitative evidence for mechanical stabilization of bainite, Mater. Sci. Technol. 12 (1996) 610–612, https://doi.org/10.1179/mst.1996.12.7.610.
[15] W. Gong, Y. Tomota, Y. Adachi, A.M. Paradowska, J.F. Kelleher, S.Y. Zhang, Effects of ausforming temperature on bainite transformation, microstructure and variant selection in nanobainite steel, Acta Mater 61 (2013) 4142–4154, https://doi.org/10.1016/j.actamat.2013.03.041.
[16] H.K.D.H. Bhadeshia, The bainite transformation: unresolved issues, Mater. Sci. Eng. A 273–275 (1999) 58–66, https://doi.org/10.1016/S0921-5093(99)00289-0.
[17] S. Chatterjee, H.-S. Wang, J. Yang, H. Bhadeshia, Mechanical stabilisation of austenite, Mater. Sci. Technol. 22 (2006) 641–644.
[18] T. Kumnorkaew, J. Lian, V. Uthaisangsuk, W. Bleck, Kinetic Model of Isothermal Bainitic Transformation of Low Carbon Steels under Ausforming Conditions, Alloys 1 (2022) 93–115, https://doi.org/10.3390/alloys1010007.
[19] N. Zolotorevsky, E. Nesterova, Y. Titovets, E. Khlusova, Modeling the effect of austenite deformation on the bainite structure parameters in low carbon microalloyed steels, Int. J. Mater. Res. 104 (2013) 337–343, https://doi.org/10.3139/146.110872.
[20] S.M.C. van Bohemen, J. Sietsma, Modeling of isothermal bainite formation based on the nucleation kinetics, Int. J. Mater. Res. 99 (2008) 739–747, https://doi.org/10.3139/146.101695.
[21] W.L. Bevilaqua, J. Epp, H. Meyer, J. Dong, H. Roelofs, A. da Silva Rocha, A. Reguly, Revealing the Dynamic Transformation of Austenite to Bainite during Uniaxial

Warm Compression through In-Situ Synchrotron X-ray Diffraction, Metals (Basel) 11 (2021) 467, https://doi.org/10.3390/met11030467.
[22] M. Veaux, J.C. Louin, J.P. Houin, S. Denis, P. Archambault, E. Aeby-Gautier, Bainitic transformation under stress in medium alloyed steels, J. Phys. IV 11 (2001), https://doi.org/10.1051/jp4:2001423. Pr4-181-Pr4-188.
[23] T.J. Su, E. Aeby-Gautier, S. Denis, Morphology changes in bainite formed under stress, Scr. Mater. 54 (2006) 2185–2189, https://doi.org/10.1016/j.scriptamat.2006.02.031.
[24] K. Nishioka, K. Ichikawa, Progress in thermomechanical control of steel plates and their commercialization, Sci. Technol. Adv. Mater. 13 (2012) 023001, https://doi.org/10.1088/1468-6996/13/2/023001.
[25] Y. Adachi, P.G. Xu, Y. Tomota, Crystallography and Kinetics of Dynamic Transformation in Steels, ISIJ Int 48 (2008) 1056–1062, https://doi.org/10.2355/isijinternational.48.1056.
[26] B. Guo, Y. Liu, J.J. Jonas, Dynamic Transformation of Two-Phase Titanium Alloys in Stable and Unstable States, Metall. Mater. Trans. A 50 (2019) 4502–4505, https://doi.org/10.1007/s11661-019-05402-x.
[27] V.A. Zaymovskiy, On the Reasons for Acceleration of the Bainite Reaction During Low-Temperature Deformation of Austenite, Phys Met Met 61 (4) (1986) 122–130.
[28] I.-E. Benrabah, Y. Brechet, G. Purdy, C. Hutchinson, H. Zurob, On the origin of the barrier in the bainite phase transformation, Scr. Mater. 223 (2023) 115076, https://doi.org/10.1016/j.scriptamat.2022.115076.
[29] M. Hillert, The Nature of Bainite, ISIJ Int 35 (1995) 1134–1140, https://doi.org/10.2355/isijinternational.35.1134.
[30] S.M.C. van Bohemen, Bainite and martensite start temperature calculated with exponential carbon dependence, Mater. Sci. Technol. 28 (2012) 487–495, https://doi.org/10.1179/1743284711Y.0000000097.
[31] J. Rodriguez-Carvajal, FULLPROF: a program for Rietveld refinement and pattern matching analysis, Satell. Meet. Powder Diffr. XV Congr. IUCr (1990) [sn].
[32] D.D. J, Effect of Alloying Additions on the Lattice Parameter of Austenite, J Iron Steel Inst 208 (1970) 469–474.
[33] A. Eres-Castellanos, L. Morales-Rivas, A. Latz, F.G. Caballero, C. Garcia-Mateo, Effect of ausforming on the anisotropy of low temperature bainitic transformation, Mater. Charact. 145 (2018) 371–380, https://doi.org/10.1016/j.matchar.2018.08.062.
[34] W. Lemos Bevilaqua, J. Epp, H. Meyer, A. Da Silva Rocha, H. Roelofs, Situ Investigation of the Bainitic Transformation from Deformed Austenite During Continuous Cooling in a Low Carbon Mn-Si-Cr-Mo Steel, Metall. Mater. Trans. A 51 (2020) 3627–3637, https://doi.org/10.1007/s11661-020-05800-6.
[35] A. Matsuzaki, H.K.D.H. Bhadeshia, H. Harada, Stress affected bainitic transformation in a FeCSi Mn alloy, Acta Metall. Mater. 42 (1994) 1081–1090, https://doi.org/10.1016/0956-7151(94)90125-2.
[36] K. Hase, C. Garcia-Mateo, H.K.D.H. Bhadeshia, Bainite formation influenced by large stress, Mater. Sci. Technol. 20 (2004) 1499–1505, https://doi.org/10.1179/026708304×6130.
[37] A. Eres-Castellanos, V. Perez-Aroca, P. Carrero-Santos, F.G. Caballero, C. Garcia-Mateo, Tuning Bainitic Microstructures by Complex Thermo-mechanical Treatments under Constant Stress, ISIJ Int 64 (2024) 316–325, https://doi.org/10.2355/isijinternational.ISIJINT-2023-148.
[38] D. Quidort, Y.J.M. Brechet, Isothermal growth kinetics of bainite in 0.5% C steels, Acta Mater. 49 (2001) 4161–4170, https://doi.org/10.1016/S1359-6454(01)00316-0.
[39] J.-O. Andersson, T. Helander, L. Höglund, P. Shi, B. Sundman, Thermo-Calc & DICTRA, computational tools for materials science, Calphad 26 (2002) 273–312.
[40] F.G. Caballero, M.K. Miller, C. Garcia-Mateo, Carbon supersaturation of ferrite in a nanocrystalline bainitic steel, Acta Mater 58 (2010) 2338–2343, https://doi.org/10.1016/j.actamat.2009.12.020.
[41] F.G. Caballero, M.K. Miller, C. Garcia-Mateo, J. Cornide, M.J. Santofimia, Temperature dependence of carbon supersaturation of ferrite in bainitic steels, Scr. Mater. 67 (2012) 846–849, https://doi.org/10.1016/j.scriptamat.2012.08.007.
[42] I. Pushkareva, J. Macchi, B. Shalchi-Amirkhiz, F. Fazeli, G. Geandier, F. Danoix, J. D.C. Teixeira, S.Y.P. Allain, C. Scott, A study of the carbon distribution in bainitic ferrite, Scr. Mater. 224 (2023) 115140, https://doi.org/10.1016/j.scriptamat.2022.115140.
[43] I.-E. Benrabah, Y. Brechet, C. Hutchinson, H. Zurob, On the origin of carbon supersaturation in bainitic ferrite, Scr. Mater. 250 (2024) 116182, https://doi.org/10.1016/j.scriptamat.2024.116182.
[44] M. Hillert, The role of interfaces in phase transformations, Mech. Phase Transform. Cryst. Solids (1969) 231–247.
[45] C.R. Hutchinson, A. Fuchsmann, Y. Brechet, The diffusional formation of ferrite from austenite in Fe-C-Ni alloys, Metall. Mater. Trans. A 35 (2004) 1211–1221, https://doi.org/10.1007/s11661-004-0295-1.
[46] A.S. Krausz, K. Krausz, Unified Constitutive Laws of Plastic Deformation, Elsevier, 1996.
[47] H. Mecking, U.F. Kocks, Kinetics of flow and strain-hardening, Acta Metall 29 (1981) 1865–1875, https://doi.org/10.1016/0001-6160(81)90112-7.
[48] J.R. Patel, M. Cohen, Criterion for the action of applied stress in the martensitic transformation, Acta Metall 1 (1953) 531–538, https://doi.org/10.1016/0001-6160(53)90083-2.
[49] H. Hu, B. Imed-Eddine, G. Xu, J. Tian, M. Zhou, Y. Bréchet, H.S. Zurob, Effect of temperature, carbon content and crystallography on the lengthening kinetics of bainitic ferrite laths, Mater. Charact. 187 (2022) 111860, https://doi.org/10.1016/j.matchar.2022.111860.
[50] H.K.D.H. Bhadeshia, S.A. David, J.M. Vitek, R.W. Reed, Stress induced transformation to bainite in Fe–Cr–Mo–C pressure vessel steel, Mater. Sci. Technol. 7 (1991) 686–698, https://doi.org/10.1179/mst.1991.7.8.686.
[51] M. Zhou, G. Xu, H. Hu, Q. Yuan, J. Tian, Comprehensive analysis on the effects of different stress states on the bainitic transformation, Mater. Sci. Eng. A 704 (2017) 427–433, https://doi.org/10.1016/j.msea.2017.08.013.
[52] M. Zhou, G. Xu, Y. Zhang, Z. Xue, The effects of external compressive stress on the kinetics of low temperature bainitic transformation and microstructure in a superbainite steel, Int. J. Mater. Res. 106 (2015) 1040–1045, https://doi.org/10.3139/146.111274.